

VisualBackProp: visualizing CNNs for autonomous driving

Mariusz Bojarski
NVIDIA Corp.
Holmdel, NJ 07735

mbojarski@nvidia.com

Anna Choromanska
Courant Institute, NYU
New York, NY 10003

achoroma@cims.nyu.edu

Krzysztof Choromanski
Google Brain Robotics
New York, NY 10011

kchoro@google.com

Bernhard Firner
NVIDIA Corp.
Holmdel, NJ 07735

bfirner@nvidia.com

Larry Jackel
NVIDIA Corp.
Holmdel, NJ 07735

ljackel@nvidia.com

Urs Muller
NVIDIA Corp.
Holmdel, NJ 07735

umuller@nvidia.com

Karol Zieba
NVIDIA Corp.
Holmdel, NJ 07735

kzieba@nvidia.com

Abstract

This paper proposes a new method, that we call VisualBackProp, for visualizing which sets of pixels of the input image contribute most to the predictions made by the convolutional neural network (CNN). The method heavily hinges on exploring the intuition that the feature maps contain less and less irrelevant information to the prediction decision when moving deeper into the network. The technique we propose was developed as a debugging tool for CNN-based systems for steering self-driving cars and is therefore required to run in real-time, i.e. it was designed to require less computation than a forward propagation. This makes the presented visualization method a valuable debugging tool which can be easily used during both training and inference. We furthermore justify our approach with theoretical arguments and theoretically confirm that the proposed method identifies sets of input pixels, rather than individual pixels, that collaboratively contribute to the prediction. Our theoretical findings stand in agreement with experimental results. The empirical evaluation shows the plausibility of the proposed approach on road data.

1. Introduction

A plethora of important real-life problems are currently addressed with CNNs [1], including image recognition [2], speech recognition [3], and natural language processing [4]. They also demonstrate excellent performance in pedestrian detection problems [5] and more recently were successfully used in car-driving systems [6, 7]. It therefore becomes increasingly important to understand the basic principles of these complicated machine learning models. One of the fundamental questions that arises when considering CNNs as well as other deep learning models is: *what made the*

trained neural network model arrive at a particular response? This question is of particular importance to end-to-end systems, where the interpretability of the system is limited. Visualization tools aim at addressing this question by identifying parts of the input image that had the highest influence on forming the final prediction by the network. It is also straightforward to think about visualization methods as a debugging tool that helps us understand if the network detects “reasonable” cues from the image to arrive at a particular decision.

The visualization method for CNNs proposed in this paper was originally developed for CNN-based systems for steering autonomous cars, though it is highly general and can be used in other applications as well. The method relies on the intuition that when moving deeper into the network, the feature maps contain less and less information which are irrelevant to the output. Thus, the feature maps of the last convolutional layer should contain the most relevant information to determine the output. At the same time, feature maps of deeper layers have lower resolution. The underlying idea of our approach is to combine feature maps containing only relevant information (deep ones) with the ones with higher resolution (shallow ones). In order to do so, starting from the feature maps of the last convolutional layer, we “backpropagate” the information about the regions of relevance while simultaneously increasing the resolution, where the backpropagation procedure is not gradient-based (as is the case for example in sensitivity-based approaches [8, 9, 10]), but instead is value-based. We call this approach VisualBackProp.

Our method provides a general tool for verifying that the predictions generated by the neural network¹, are based on reasonable optical cues in the input image. In case of au-

¹In the case of our end-to-end system for steering an autonomous car, a prediction is the steering wheel angle.

onomous driving these can be lane markings, other cars, or edges of the road. Our visualization tool runs in real time and requires less computation than forward propagation.

In the theoretical part of this paper we first provide a rigorous mathematical analysis of the contribution of input neurons to the activations in the last layer that relies on network flows. We propose a quantitative measure of that contribution. We then show that our algorithm finds for each neuron the approximated value of that measure. In fact our method can be modified to get the accurate value of the contribution, but since the modification leads to a slower algorithm and our experimental results do not show any difference between both variants, we present the results that are obtained for a faster variant.

The paper is organized as follows: Section 2 discusses relevant literature, Section 3 describes our approach, Section 4 provides a theoretical analysis of the approach, Section 5 presents empirical verification and Section 6 concludes the paper with a brief discussion.

2. Related work

A notable approach [11] for understanding CNNs with max-pooling and rectified linear units (ReLU) through visualization uses deconvolutional neural network [12] attached to the convolutional network of interest. This approach maps the feature activity in intermediate layers of a previously trained CNN back to the input pixel space via successively repeated operations of i) unpooling, where switch variables are used to record the locations of maxima within each pooling region, ii) rectification, and iii) filtering, where these stages are performed by the deconvolutional network. The authors focus on a supervised learning task of image classification and show that the proposed visualization provides insights into the operation of the classifier and the function of intermediate feature layers. They identify layers responding to corners and other edge/color conjunctions, layers that focus on more complex invariances like similar textures, as well as layers that show significant variation and are more class-specific. These observations help to diagnose the network’s architecture, for example by detecting layers which poorly represent certain bands of frequencies or those inducing aliasing artifacts. The authors also use their visualization technique with respect to the first layer to observe the evolution of features during training. Since this method identifies structures within each patch that stimulate a particular feature map, it differs from previous approaches [13] which instead identify patches within a data set that stimulate strong activations at higher layers in the model. The method can also be interpreted as providing an approximation to partial derivatives with respect to pixels in the input image [9]. As explained by the authors, the approach is somewhat similar to back-propagating a single strong activation, i.e. comput-

ing $\frac{\partial h}{\partial X}$ (h is the element of the feature map with strong activation and X is the input image), instead of the usual gradient. ReLU is imposed independently and contrast normalization operations are omitted. One of the shortcomings of the method is that it enables the visualization of only a single activation in a layer (all other activations are set to zero). Nevertheless, their sensitivity analysis reveals that the proposed visualization accurately represents the input pattern that stimulates the given feature map in the model. There also exist other techniques for inverting a modern large convolutional network with another network, e.g. a method based on up-convolutional architecture [14], where as opposed to the previously described deconvolutional neural network [11], the up-convolutional network is trained. This method inverts deep image representations and obtains reconstructions of an input image from each layer.

Another approach [15] addressing the problem of understanding classification decisions by pixel-wise decomposition of non-linear classifiers proposes a methodology called layer-wise relevance propagation (LRP), where the prediction is back-propagated without using gradients such that the relevance of each neuron is redistributed to its predecessors through a particular message-passing scheme. The method relies on the conservation principle which ensures that the network output activity is fully redistributed through the layers of a neural network model onto the input variables. This approach allows the visualization of the contribution of single pixels to the predictions of a previously trained network as heatmaps. The method applies to a broader class of networks than CNNs. The LRP technique was later extended to Fisher Vector classifiers [16] and also used to explain predictions of CNNs in NLP applications [17]. The fundamental difference between the LRP approach and the deconvolution method lies in how the responses are projected towards the inputs. The latter approach solves the optimization problems to reconstruct the image input while the former approach aims to reconstruct the classifier decision (the details are well-explained in [15]). Furthermore, a comparison of LRP with the deconvolution method and the sensitivity-based approach, (sensitivity-based methods, e.g. [8, 9, 10] compute scores based on partial derivatives at the given sample and can be applied to reveal how the classifier works in different parts of the input domain), using an evaluation based on region perturbation can be found in [18]. An approach similar in spirit to LRP uses contribution propagation [19], where the authors calculate the contributions of high-level features using a previously known technique [20] and then work backwards from the features to the network’s input determining the relative contribution of each node to its parent nodes.

Understanding CNNs can also be done by visualizing output units as distributions in the input space via output unit sampling [21]. However, computing relevant statis-

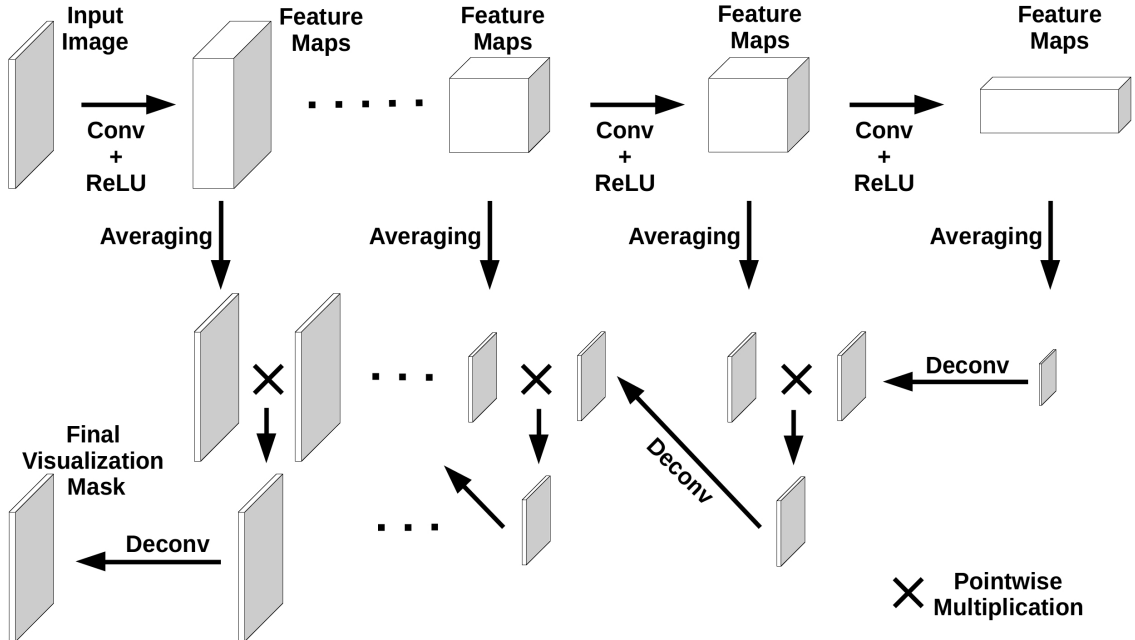


Figure 1. Block diagram of the VisualBackProp method. The feature maps after each ReLU layer are averaged. The averaged feature map of the last convolutional layer is scaled-up via deconvolution and multiplied by the averaged feature map from the previous layer. The resulting intermediate mask is again scaled-up and multiplied. This process is repeated until we reach the input.

tics of the obtained distribution is often difficult. Furthermore this technique cannot be applied to deep architectures based on auto-encoders as opposed to the subsequent work [22, 23]. In their work the authors visualize what is activated by the unit in an arbitrary layer of a CNN in the input space (of images) via an activation maximization procedure that looks for input patterns of a bounded norm that maximize the activation of a given hidden unit (this is done using gradient ascent). The method extends previous approaches [24] and can also be used to trace invariance manifolds for each of the hidden units. The gradient-based visualization method [23] can also be viewed as a generalization of the deconvolutional network reconstruction procedure [11] as shown in subsequent work [9]. The requirement of careful initialization limits the method [11]. The approach was applied to Stacked Denoising Auto-Encoders, Deep Belief Networks and later on to CNNs [9]. The latter work also proposes a technique for computing a class saliency map from a CNN, specific to a given image and class. Instead of projecting back convolutional features to the input space [11], they perform the projection from the fully connected layers of the network.

Finally, understanding CNNs in the context relevant to this paper was also done in the past by characterizing their intriguing and often counter-intuitive properties [25, 26], quantifying the importance of input variables using a neural network model [27, 28], extracting the rules learned by the decision tree model that is fitted to the function learned by the neural network model [29], applying kernel analy-

sis to understand the layer-wise evolution of the representation in a deep network [30], analyzing the visual information contained in deep image representations by looking at the inverse representations [31], or visualizing particular neurons or neuron layers [2, 32]. There are also more generic tools for explaining individual classification decisions of any classification method for single data instances, like the framework based on local explanation vectors [8] which yields the features relevant for the prediction at the data points of interest and takes into consideration local peculiarities that are neglected in the global view, for example, due to cancellation effects.

To the best of our knowledge, the existing visualization techniques for deep learning discussed above lack any theoretical guarantees, though they often stem from a firm theoretical intuition and some of them provide a theoretical description. We instead provide such guarantees for our method.

3. Visualization method

As mentioned before, our method combines feature maps from deep convolutional layers that contain mostly relevant information, but are low-resolution, with the feature maps of the shallow layers that have higher resolution but also contain more irrelevant information. This is done by “back-propagating” the information about the regions of relevance while simultaneously increasing the resolution. The back-propagation is value-based. We call this approach VisualBackProp to emphasize that we “back-

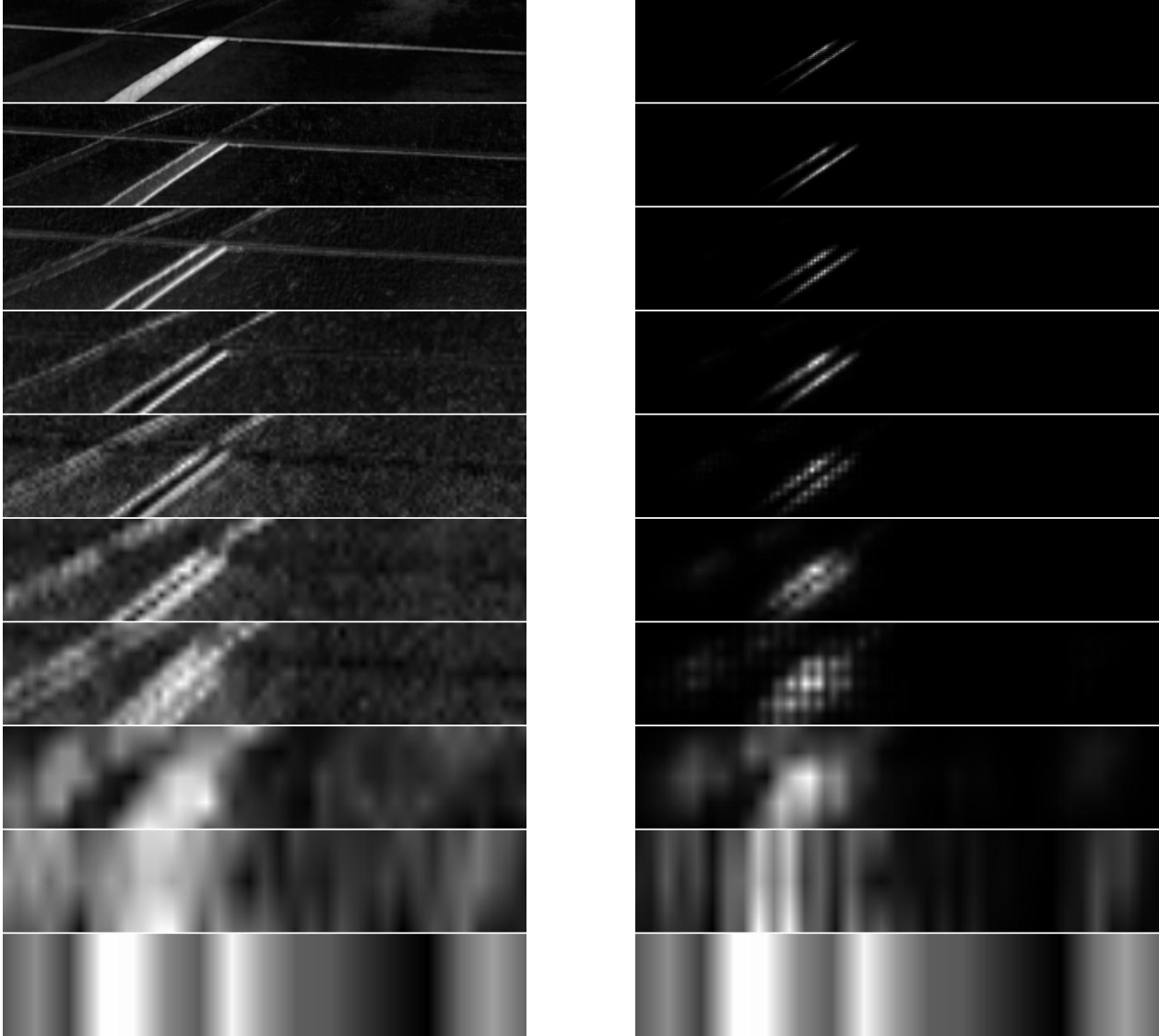


Figure 2. **Left:** Averaged feature maps of all convolutional layers from the input (top) to the output (bottom). **Right:** Corresponding intermediate masks. The top one is the final result.

propagate” values (images) instead of gradients. We explain the method in details below.

The block diagram of the proposed visualization method is shown in Figure 1. The method utilizes the forward propagation pass, which is already done to obtain a prediction, i.e. we do not add extra forward passes. The method then uses the feature maps obtained after each ReLU layer (thus these feature maps are already thresholded). In the first step, the feature maps from each layer are averaged, resulting in a single feature map per layer. Next, the averaged feature map of the deepest convolutional layer is scaled up to the size of the feature map of the previous layer. This is done using deconvolution with filter size and stride that are the same as the ones used in the deepest convolutional layer (for deconvolution we always use the same filter size and

stride as in the convolutional layer which outputs the feature map that we are scaling up with the deconvolution). In deconvolution, all weights are set to 1 and biases to 0. The obtained scaled-up averaged feature map is then point-wise multiplied by the averaged feature map from the previous layer. The resulting image is again scaled via deconvolution and multiplied by the averaged feature map of the previous layer exactly as described above. This process continues all the way to the network’s input as shown in Figure 1. In the end, we obtain a mask of the size of the input image, which we normalize to the range $[0, 1]$.

The process of creating the mask is illustrated in Figure 2. On the left side the figure shows the averaged feature maps of all the convolutional layers from the input (top) to the output (bottom). On the right side it shows the cor-

responding intermediate masks. Thus on the right side we show step by step how the mask is being created when moving from the network’s output to the input. Comparing the two top images clearly reveals that many details were removed in order to obtain the final mask. Finally, Figure 3 shows the mask overlaid on the input image.

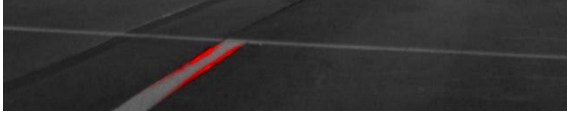


Figure 3. Input image with the mask overlaid in red.

4. Theoretical analysis

We now present theoretical guarantees for the algorithm. All proofs are given in the Supplementary Material. It is worthwhile to emphasize that our theoretical analysis is not about computing the sensitivity of any particular cost function with respect to changes of values of particular input neurons. So we will not focus on computing gradients. The reason for that is that even if these gradients are large, the actual contribution of the neuron might be small. Instead our proposed method is measuring the actual contribution that takes into account the “collaborative properties” of particular neurons. This is measured by the ability of particular neurons to substantially participate in these weighted inputs to neurons in consecutive layers that themselves have higher impact on the form of the ultimate feature maps than others.

Let’s consider a convolutional neural network \mathcal{N} with L convolutional layers that we index from 1 to L and ReLU nonlinear mapping with biases $-b_v$, where v stands for a neuron of the network. We assume that no pooling mechanism is used. For simplicity we assume that the strides are equal to one. However, the entire analysis can be repeated for arbitrary stride values. We denote by f_l the number of feature feature maps of the l^{th} layer, by $a_l \times b_l$ the shape of the kernel applied in the l^{th} convolutional layer and by s_l the number of neurons in each feature map of the l^{th} convolutional layer. We will denote by $a(v)$ the activation of the neuron v .

For a CNN with learned weights and biases we think about the inference phase as a network flow problem, where source nodes are the neurons of the input layer ($l = 0$) and sinks are nodes of the output layer (output of the last convolutional layer). In that setting the flow is (dis-)amplified when it travels along edges and furthermore some fraction of the flow is lost in certain nodes of the network (due to biases).

Our first observation relates the inference phase to the aforementioned flow problem on the sparse multipartite graph with $L + 1$ parts A_0, A_1, \dots, A_L and where vertex v in the part A_{i-1} has $a_i b_i f_i$ neighbors in part A_i .

Lemma 1 *The inference phase in the model above is equivalent to the network flow model on a multipartite graph with parts A_1, \dots, A_L , where each edge has a weight defining the amplification factor for the flow traveling along this edge. In each node v the flow of value $\min(z_v, b_v)$ is lost, where z_v is the incoming flow and where vertex v in the part A_{i-1} has $a_i b_i f_i$ neighbors in part A_i .*

Different parts A_i above correspond to different convolutional layers (A_0 corresponds to the input layer). From now on we will often implicitly transition from the neural network description to the graph theory and vice versa using the above mapping.

The flow-formulation of the problem is convenient since it will enable us to quantitatively measure the contribution of neurons from the input layer to the activations of neurons in the last convolutional layer. Before we propose a definition of that measure, let us consider a simple scenario, where no nonlinear mapping is applied. That neural network model would correspond to the network flow for multipartite graphs described above, but with no loss of the flow in the nodes of the network.

In that case different input neurons act independently. For each node X in A_0 the total flow value received by A_L is obtained by summing over all paths P from X to A_L the expressions of the form $f(X) \prod_{e \in P} w_e$, where w_e stands for the weight of an edge e and $f(X)$ is the value of the input flow to X (see Figure 4). This observation motivates the following definition:

Definition 1 (ϕ -function for CNNs with no biases)

Consider the neural network architectures \mathcal{N} described above but with no biases. Then the contribution of the input neuron X to the last layer of feature maps is given as:

$$\phi^{\mathcal{N}}(X) = v(X) \sum_{P \in \mathcal{P}} \prod_{e \in P} w_e, \quad (1)$$

where $v(X)$ is the value of X and \mathcal{P} is a family of paths from X to A_L in the corresponding multipartite graph.

In our setting the biases need to be taken into account, but the definition above suggests how to do this: We transform our CNN with biases \mathcal{N} to the one without biases $\tilde{\mathcal{N}}$, but with corrected weights of edges. We do it in such a way that the following property will be satisfied:

For every neuron X and every incoming edge e_0 the input flow f_0 along e_0 is replaced by $a(X) \frac{f_0}{\sum_e f(e)}$, where the summation goes over all incoming edges e . $f(e)$ stands for the input flow along e and $a(X)$ is an activation of X in the original network.

Note that this network is equivalent to the original one, i.e. it produces the same activations for all its neurons as the original one. Furthermore, the property above just says that

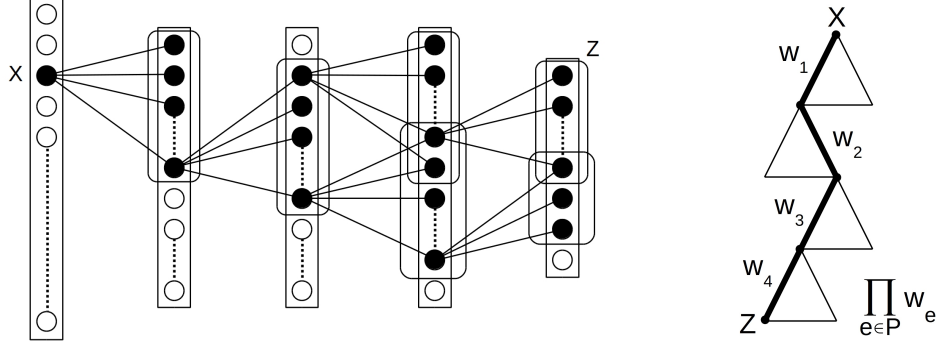


Figure 4. Convolutional architecture with no biases. The contribution of each neuron can be computed by summing the contribution along different paths originating at X and ending in the last layer. The contribution from each path is proportional to the product of the weights of edges belonging to this path.

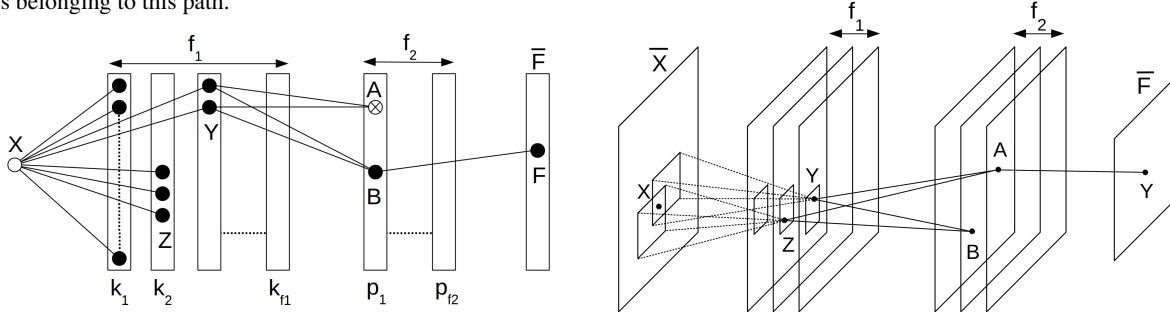


Figure 5. **Right:** General CNN \mathcal{N} with biases. **Left:** Corresponding multipartite graph. Dead nodes, i.e. nodes that do not transmit any flow (corresponding to neurons with zero activation), are crossed.

the contribution of the given input flow f to the activation of X is proportional to the value of the flow (this is a desirable property since the applied nonlinear mapping is a ReLU function). It also captures the observation that if the flow is large, but the activation is small, the contribution might be also small since even though the flow contributes substantially, it contributes to an irrelevant feature.

Lemma 2 *The above network $\tilde{\mathcal{N}}$ can be obtained from the original one \mathcal{N} by multiplying each weight w_e of an edge $e = (n_1, n_2)$ by $c(e) = \frac{a_e}{z(e)}$, where a_e stands for the activation of the neuron n_1 and $z(e)$ is a weighted input to the neuron n_2 .*

Since we know how to calculate the contribution of each input neuron to the convolutional network in the setting without biases and we know how to translate any general convolutional neural network \mathcal{N} (see: Figure 5) to the equivalent one $\tilde{\mathcal{N}}$ without biases, we are ready to give a definition of the contribution of each input neuron in the general network \mathcal{N} .

Definition 2 (ϕ -function for general CNNs) *Consider the general neural network architecture described above. Then the contribution of the input neuron X to the last layer of feature maps is given as:*

$$\phi^{\mathcal{N}}(X) = \phi^{\tilde{\mathcal{N}}}(X), \quad (2)$$

where $\tilde{\mathcal{N}}$ stands for the counterpart of \mathcal{N} with no biases described above.

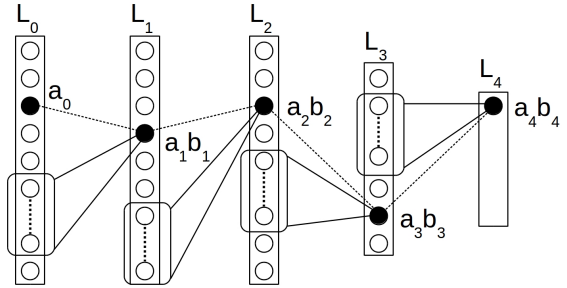


Figure 6. The contribution of any given input neuron X along a particular path P in the general CNN \mathcal{N} is equal to the product $\prod_{e \in P} \frac{a_i w_i}{a_i + b_i}$, where a_i s are the activations on the path and b_i s are the corresponding biases.

We are now ready to express the contribution of the neuron X in \mathcal{N} explicitly in terms of the parameters of \mathcal{N} .

Lemma 3 *For an input neuron X function $\phi^{\mathcal{N}}(X)$ is defined as (Figure 6):*

$$\phi^{\mathcal{N}}(X) = v(X) \sum_{P \in \mathcal{P}} \prod_{e \in P} \frac{a_e}{a_e + b_e} w_e, \quad (3)$$

where $v(X)$ is the value of pixel X , \mathcal{P} is a family of paths from X to A_L in the corresponding multipartite graph, b_e is a bias in the second neuron of e and a_e s are as above.

Note that in the network with no biases one can set $b_e = 0$ and obtain the results introduced before the formula involving sums of weights' products.

We prove the following results (borrowing the notation introduced before) by connecting our previous theoretical analysis with the algorithm.

Theorem 1 *For a fixed CNN \mathcal{N} considered in this paper there exists a universal constant $c > 0$ such that the values of the input neurons computed by VisualBackProp are of the form:*

$$\phi_{VBP}^{\mathcal{N}}(X) = c \cdot v(X) \sum_{P \in \mathcal{P}} \prod_{e \in P} a_e. \quad (4)$$

The formula on $\phi_{VBP}^{\mathcal{N}}(X)$ is similar to the one on $\phi^{\mathcal{N}}(X)$. Note that the latter one can be obtained from the former one by multiplying each term of the inner products by $\frac{w_e}{a_e + b_e}$ and then rescaling by a multiplicative factor of $\frac{1}{c}$. Rescaling does not have any impact on quality since it is conducted in exactly the same way for all the input neurons. In the next section we show empirically that $\phi_{VBP}^{\mathcal{N}}(X)$ works very well as a measure of contribution. Thus it might be the case that for the considered setting $\phi^{\mathcal{N}}(X)$ is a near-monotonic function of $\phi_{VBP}^{\mathcal{N}}(X)$.

In fact, the exact implementation of the score $\phi^{\mathcal{N}}(X)$ can be obtained by a straightforward modification of the presented algorithm *VisualBackProp* (weighted copying of the activation of the neuron before multiplying by a mask as opposed to the unweighted one). However such an algorithm is slower and our experimental results did not show any visible difference between the two approaches thus we present the faster method.

5. Experiments

We demonstrate the usefulness of VisualBackProp with the example of end-to-end learning for autonomous driving using a network and data similar to those described in [6].

The experiments are performed on one of Udacity's self-driving car data sets [33]. This data set contains images from three front-facing cameras (left, center, and right) and measurements such as speed and steering wheel angle, recorded from the vehicle driving on the road. The measurements and images are recorded with different sampling rates and are independent, thus they require synchronization before they can be used for training neural networks. For the purpose of this paper, we pre-process the data with the following operations: i) synchronizing images with measurements from the vehicle, ii) selecting only center camera images, iii) selecting images where the car speed is above 5 m/s, iv) converting images to gray scale, and v) cropping the lower part of the images to a 640×135 size. As a result, we obtain a data set with 210 K images with corresponding steering wheel angles (speed is not used), where the first

190 K examples are used as for training and the remaining 20 K examples are used for testing. We train the CNN to predict steering wheel angles based on the images from the training data set. The network architecture is defined in Table 1. The network is trained with stochastic gradient descent (SGD) and the mean squared error (MSE) cost function for 32 epochs.

Layer	Output size	Filter size	Stride
conv	32x123x638	3x3	1x1
conv	32x61x318	3x3	2x2
conv	48x59x316	3x3	1x1
conv	48x29x157	3x3	2x2
conv	64x27x155	3x3	1x1
conv	64x13x77	3x3	2x2
conv	96x11x75	3x3	1x1
conv	96x5x37	3x3	2x2
conv	128x3x35	3x3	1x1
conv	128x1x17	3x3	2x2
FC	1024	-	-
FC	512	-	-
FC	1	-	-

Table 1. Architecture of the neural network used in the experiments. Each layer except for the last fully-connected layer is followed by ReLU. Each convolution layer is preceded by a batch normalization layer.

Our VisualBackProp method was applied on selected images during training. The obtained masks for an exemplary image are shown in Figure 7. The figure captures how the CNN gradually learns to recognize visual cues relevant for steering a car (lane markings in this case) as the learning algorithm proceeds.

We next demonstrate the usefulness of the proposed method for analyzing the behavior of a trained neural network. We do this by overlaying VisualBackProp masks on various input images of the test data. Examples are shown in Figures 8–12. For each image we report error defined as a difference between the actual and predicted steering wheel angle (SWA) in degrees.

Images in Figure 8 illustrate that the CNN learned to recognize lane markings. Lane markings are among the most relevant visual cues for steering a car. This helps us understand how the neural network operates and makes it less of a black box.

Figure 9 captures how the CNN responds to shadows on the image. One can see that the network still detects lane markings but only between the shadows, where they are visible. This indicates that we need more diverse data with shadows such that the network would learn to ignore them.

Figure 10 shows two consecutive frames where on the second one, the lane marking on the left side of the road disappears. We can see that the CNN starts following the lane marking on the right when the previously followed left marking suddenly disappears: the right marking becomes

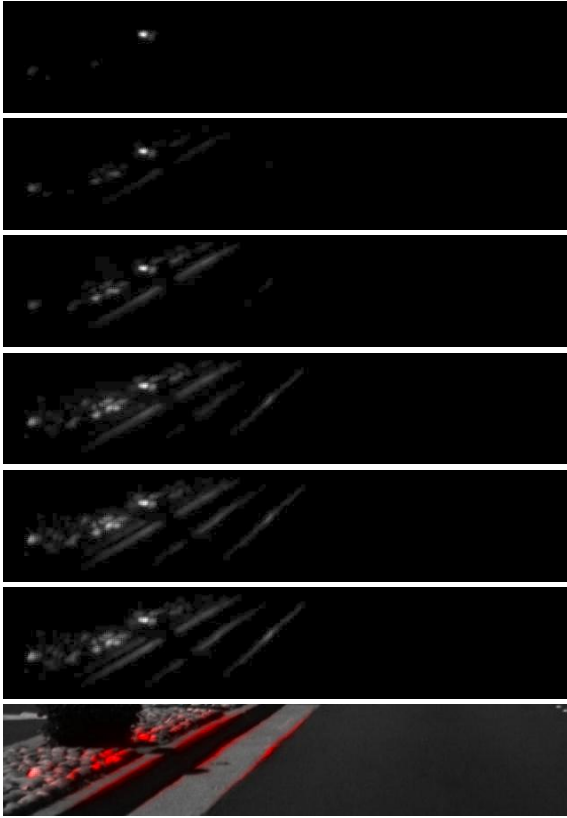


Figure 7. Visualizing the training of the CNN with the VisualBack-Prop method: images from top to bottom show the mask after 0.1, 0.5, 1, 4, 16, and 32 epochs. Over time the network learns to detect more relevant cues for the task from the training data. The last picture shows input image with the mask overlaid in red.

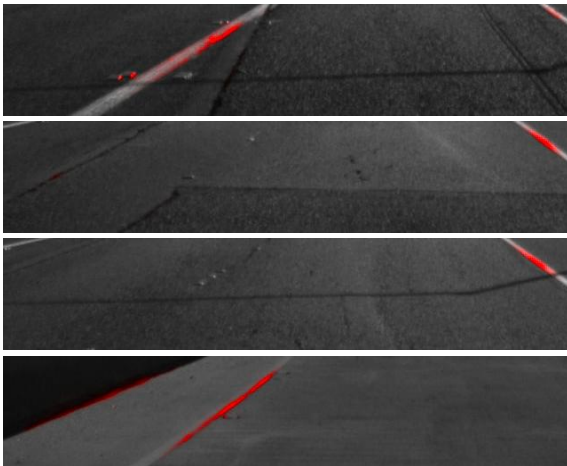


Figure 8. Input test images with the corresponding masks overlaid in red. The network is detecting lane markings which are the most relevant cues for the task of lane following. The errors are (from the top): 0.01, 1.90, 4.35, and -1.32 degrees of SWA.

the most relevant visual cue for steering a car. It is another strong indication that the network learned the task correctly by using the most relevant visual cues that are available at any given time.

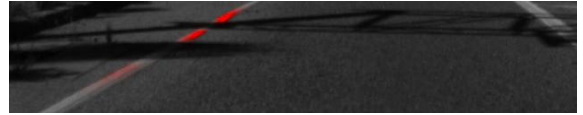


Figure 9. Input test image with the mask overlaid in red. Shadows affect network's perception. The error is -0.83 degrees of SWA.

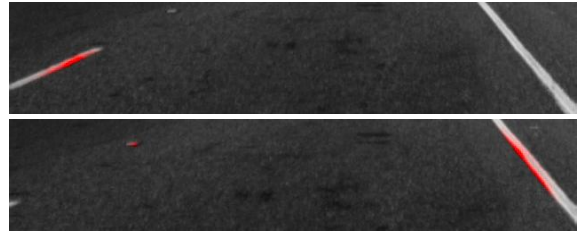


Figure 10. Two consecutive frames with the corresponding masks overlaid in red. The network is switching from the left to the right lane marking to be able to steer the car. The errors are (from the top): -3.19 and -3.21 degrees of SWA.

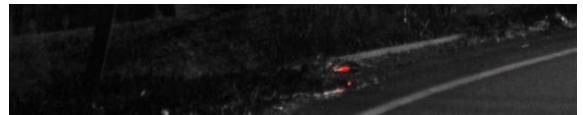


Figure 11. Input test image with the mask overlaid in red. The network is detecting wrong features from the image which results in high prediction error of 68.64 degrees of SWA.

Figure 11 shows a case where the network makes a mistake. It demonstrates the situation when the CNN is not looking at the lane marking but some random objects outside the road. This network's mistake is not unexpected as there is only a small amount of similar examples (sharp turns) in the training data set.

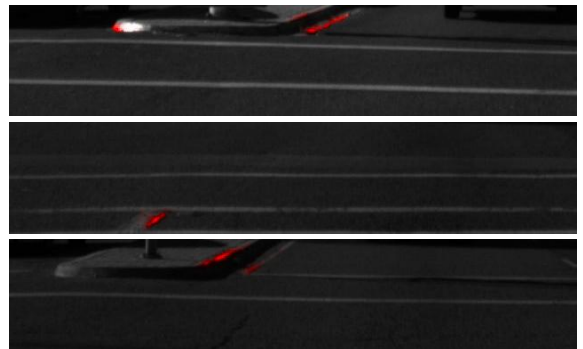


Figure 12. Input test images with the corresponding masks overlaid in red. The network learned to ignore horizontal lines as they do not provide relevant information for the task of lane following. The errors are (from the top): -5.41 , -3.39 , and -2.21 degrees of SWA.

Finally, in Figure 12 we show three examples demonstrating that the CNN has learned to ignore horizontal lane markings as they are not relevant for steering a car. It is an interesting observation, particularly in the view of the fact that the CNN was trained only with the images and the steering wheel angles as the training signal. The neural network was able to learn which visual cues are relevant for the

task of steering the car from the steering wheel angle alone.

6. Conclusions

In this paper we propose a new method for visualizing the regions of the input image that have the highest influence on the output of a CNN. The presented approach is computationally efficient which makes it a feasible method for real-time applications as well as for the analysis of large data sets. We provide theoretical justification for the proposed method and empirically show on the task of autonomous driving (a challenging problem for modern artificial intelligence) that it is a valuable diagnostic tool for CNNs.

References

- [1] Y. LeCun, B. Boser, J. S. Denker, D. Henderson, R. E. Howard, W. Hubbard, and L. D. Jackel. Backpropagation applied to handwritten zip code recognition. *Neural Comput.*, 1(4):541–551, 1989. 1
- [2] A. Krizhevsky, I. Sutskever, and G. E. Hinton. Imagenet classification with deep convolutional neural networks. In *NIPS*. 2012. 1, 3
- [3] O. Abdel-Hamid, A.-r. Mohamed, H. Jiang, and G. Penn. Applying convolutional neural networks concepts to hybrid NN-HMM model for speech recognition. In *ICASSP*, 2012. 1
- [4] J. Weston, S. Chopra, and K. Adams. #tagspace: Semantic embeddings from hashtags. In *EMNLP*, 2014. 1
- [5] A. Angelova, A. Krizhevsky, V. Vanhoucke, A. Ogale, and D. Ferguson. Real-time pedestrian detection with deep network cascades. In *BMVC*, 2015. 1
- [6] M. Bojarski, D. Del Testa, D. Dworakowski, B. Firner, B. Flepp, P. Goyal, L. D. Jackel, M. Monfort, U. Muller, J. Zhang, X. Zhang, J. Zhao, and K. Zieba. End to end learning for self-driving cars. *CoRR*, abs/1604.07316, 2016. 1, 7
- [7] C. Chen, A. Seff, A. L. Kornhauser, and J. Xiao. Deep-driving: Learning affordance for direct perception in autonomous driving. In *ICCV*, 2015. 1
- [8] D. Baehrens, T. Schroeter, S. Harmeling, M. i Kawanabe, K. Hansen, and K.-R. Müller. How to explain individual classification decisions. *J. Mach. Learn. Res.*, 11:1803–1831, 2010. 1, 2, 3
- [9] K. Simonyan, A. Vedaldi, and A. Zisserman. Deep inside convolutional networks: Visualising image classification models and saliency maps. In *Workshop Proc. ICLR*, 2014. 1, 2, 3
- [10] P. M. Rasmussen, T. Schmah, K. H. Madsen, T. E. Lund, S. C. Strother, and L. K. Hansen. Visualization of nonlinear classification models in neuroimaging - signed sensitivity maps. *BIOSIGNALS*, pages 254–263, 2012. 1, 2
- [11] M. D. Zeiler and R. Fergus. Visualizing and understanding convolutional networks. In *ECCV*, 2014. 2, 3
- [12] M. D. Zeiler, G. W. Taylor, and R. Fergus. Adaptive deconvolutional networks for mid and high level feature learning. In *ICCV*, 2011. 2
- [13] R. Girshick, J. Donahue, T. Darrell, and J. Malik. Rich feature hierarchies for accurate object detection and semantic segmentation. In *CVPR*, 2014. 2
- [14] A. Dosovitskiy and T. Brox. Inverting visual representations with convolutional networks. In *CVPR*, 2016. 2
- [15] S. Bach, A. Binder, G. Montavon, F. Klauschen, K.-R. Müller, and W. Samek. On pixel-wise explanations for non-linear classifier decisions by layer-wise relevance propagation. *PLOS ONE*, 10(7):e0130140, 2015. 2
- [16] S. Bach, A. Binder, G. Montavon, K.-R. Müller, and W. Samek. Analyzing classifiers: Fisher vectors and deep neural networks. In *CVPR*, 2016. 2
- [17] L. Arras, F. Horn, G. Montavon, K.-R. Müller, and W. Samek. Explaining predictions of non-linear classifiers in NLP. In *ACL Workshop on Representation Learning for NLP*, 2016. 2
- [18] W. Samek, A. Binder, G. Montavon, S. Bach, and K.-R. Müller. Evaluating the visualization of what a deep neural network has learned. *CoRR*, abs/1509.06321, 2015. 2
- [19] W. Landecker, M. I. D. Thomure, L. M. A. Bettencourt, M. Mitchell, G. T. Kenyon, and S. P. Brumby. Interpreting individual classifications of hierarchical networks. In *CIDM*, 2013. 2
- [20] B. Poulin, R. Eisner, D. Szafron, P. Lu, R. Greiner, D. S. Wishart, A. Fyshe, B. Percy, C. Macdonell, and J. Anvik. Visual explanation of evidence with additive classifiers. In *IAAI*, 2006. 2
- [21] G. E. Hinton, S. Osindero, and Y.-W. Teh. A fast learning algorithm for deep belief nets. *Neural Comput.*, 18(7):1527–1554, 2006. 2
- [22] D. Erhan, A. Courville, and Y. Bengio. Understanding representations learned in deep architectures. Technical Report 1355, University of Montreal, 2010. 3
- [23] D. Erhan, Y. Bengio, A. Courville, and P. Vincent. Visualizing higher-layer features of a deep network. Technical Report 1341, University of Montreal, 2009. 3
- [24] P. Berkes and L. Wiskott. On the analysis and interpretation of inhomogeneous quadratic forms as receptive fields. *Neural Computation*, 18(8):1868–1895, 2006. 3
- [25] C. Szegedy, W. Zaremba, I. Sutskever, J. Bruna, D. Erhan, I. J. Goodfellow, and R. Fergus. Intriguing properties of neural networks. In *ICLR*, 2014. 3
- [26] I. J. Goodfellow, J. Shlens, and C. Szegedy. Explaining and harnessing adversarial examples. *CoRR*, abs/1412.6572, 2014. 3
- [27] M. Gevrey, I. Dimopoulos, and S. Lek. Review and comparison of methods to study the contribution of variables in artificial neural network models. *Ecological Modelling*, 160(3):249–264, 2003. 3

- [28] J. D. Olden, M. K. Joy, and R. G. Death. An accurate comparison of methods for quantifying variable importance in artificial neural networks using simulated data. *Ecological Modelling*, 178(34):389 – 397, 2004. 3
- [29] R. Setiono and H. Liu. Understanding neural networks via rule extraction. In *IJCAI*, 1995. 3
- [30] G. Montavon, M. L. Braun, and K.-R. Müller. Kernel analysis of deep networks. *J. Mach. Learn. Res.*, 12:2563–2581, 2011. 3
- [31] A. Mahendran and A. Vedaldi. Understanding deep image representations by inverting them. In *CVPR*, 2015. 3
- [32] J. Yosinski, J. Clune, A. M. Nguyen, T. Fuchs, and H. Lipson. Understanding neural networks through deep visualization. *CoRR*, abs/1506.06579, 2015. 3
- [33] Udacity self driving car dataset 3-1: El camino. 7

VisualBackProp: visualizing CNNs for autonomous driving (Supplementary Material)

7. Proof of Lemma 1

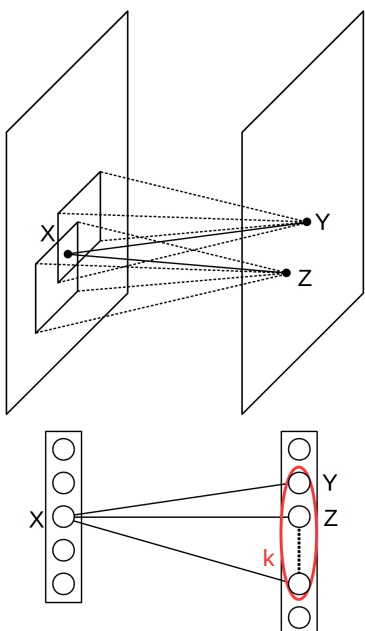


Figure 13. Neuron X is covered by patches corresponding to selected neurons in the consecutive layer. In the corresponding multipartite graph node X is adjacent to selected vertices in the next part and transports the flow to them.

Proof: As we have explained in the main body of the paper, we will identify the source-nodes for the flow problem with input neurons and the sink-nodes with the neurons of the last convolutional layer. Parts A_1, \dots, A_L are the sets of nodes in the corresponding convolutional layers (observe that indeed there are no edges between nodes in A_i s since

there are no edges between neurons in feature maps associated with the fixed convolutional layer). Part A_0 represents the input layer. Each source-node $v \in A_{i-1}$ sends $a(v)$ units of flow along edges connecting it with nodes in part A_i . This is exactly the amount of the input flow $f(v)$ to the node v with flow of value $\min(f_v, b_v)$ deducted (due to the ReLU nonlinear mapping). The activations of neurons in the last convolutional layer can be represented in that model as the output flows of the nodes from A_L . Note that for a fixed neuron v in the $(i-1)^{th}$ convolutional layer and fixed feature map in the consecutive convolutional layer (here the 0^{th} layer is the input layer) the kernel of size $a_i \times b_i$ can be patched in $a_i b_i$ different ways (see: Figure 13) to cover neuron v (this is true for all but the “borderline neurons” which we can neglect without loss of generality; if one applies padding mechanism the “borderline neurons” do not exist at all). Thus the total number of connections of v to the neurons in the next layer is $a_i b_i f_i$. A similar analysis can be conducted if v is an input neuron. That completes the proof. \square

8. Proof of Lemma 2

Proof: Assume that $e = (A, B)$, where A is a first node of the edge and B is second one. Note that from the definition of $\tilde{\mathcal{N}}$ for an input flow f , the flow of value $a_e \frac{f}{F}$ is transmitted by B , where F stands for the total input flow to B . Note also that $F = z(e)$. Furthermore $f = \tilde{f} w_e$, where \tilde{f} is the original value of f before amplification obtained by passing that flow through an edge e . Thus the flow \tilde{f} output by A is multiplied by $w_e \frac{a_e}{z_e}$ and output by B . Thus one can set: $c(e) = \frac{a_e}{z_e}$. That completes the proof. \square

9. Proof of Lemma 3

Proof: Straightforward from the formula on $\phi^{\tilde{\mathcal{N}}}(X)$ and derived formula on transforming weights of $\tilde{\mathcal{N}}$ to obtain $\tilde{\mathcal{N}}$. \square

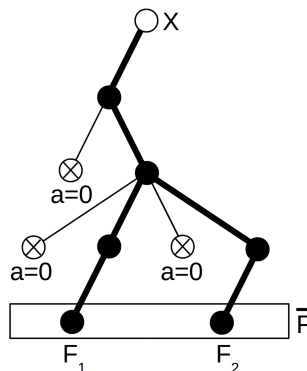


Figure 14. The family of paths from the input neuron X to output neurons F_1 and F_2 in the last set of feature maps \bar{F} . Crossed nodes correspond to neurons with zero activation. Paths containing these nodes do not contribute to \bar{F} .

10. Proof of Theorem 1

Proof: Note that averaging over different feature maps in the fixed convolutional layer with f_i feature maps that is conducted by *VisualBackProp* is equivalent to summing over paths with edges in different feature maps of that layer (up to a multiplicative constant $\frac{1}{f_i}$.) Furthermore, adding contributions from different patches covering a fixed neuron X is equivalent to summing over all paths that go through X . Thus computed expression is proportional to the union of products of activations (since in the algorithm after re-sizing the masks are pointwise multiplied) along paths from the given input neuron X to all the neurons in the last set of feature maps. That leads to the proposed formula. Note that the formula automatically gets rid of all the paths that lead to a neuron with null activation since these paths do not contribute to activations in the last set of feature maps (see: Figure 14). \square